



Light propagation along a helical waveguide: variational approach

Aleksandra I. Strinić^{1,3} · Najdan B. Aleksić^{1,2,3} · Milivoj R. Belić³ · Milan S. Petrović⁴

Received: 31 October 2019 / Accepted: 29 April 2020 / Published online: 1 June 2020
© Springer Science+Business Media, LLC, part of Springer Nature 2020

Abstract

We investigate numerically and analytically light propagation in a single spiral waveguide formed in a nonlinear dielectric medium, in the regime of low spatial frequency of the waveguide rotation. We present a general variational approach for computing soliton parameters analytically, which includes various types of nonlinearity. In the particular case of media with cubic-quintic nonlinearity, analytical expressions found are in very good agreement with the numerical findings.

Keywords Light propagation · Spiral waveguide · Variational approach

1 Introduction

Spatial optical solitons are self-localized wave packets which propagate in a nonlinear medium without changing their internal structure, originating from a robust balance between dispersion and nonlinearity (Kivshar and Agrawal 2003). They usually propagate along a well-defined propagation direction, but in general, the beam propagation need not proceed along a straight line. More interesting dynamics can be found in rotating propagation systems, because the centripetal force modifies the interaction with the medium or other beams, as well as the effect of external potentials present.

Solitons in rotating periodic lattices were investigated in Cuevas et al. (2007), Longhi (2007), Jia and Fleischer (2009), Sakaguchi and Malomed (2009); it was shown that the nonlinear light propagation in a rotating waveguide array couples Bloch modes both within and between bands, and that these non-inertial effects can lead to mode conversion,

This article is part of the Topical Collection on Advanced Photonics Meets Machine Learning.

Guest edited by Goran Gligoric, Jelena Radovanovic and Aleksandra Maluckov.

✉ Aleksandra I. Strinić
strinic@ipb.ac.rs

¹ Institute of Physics, University of Belgrade, P.O. Box 68, 11080 Belgrade, Serbia

² Moscow State Technological University “STANKIN”, Moscow, Russia

³ Texas A&M University at Qatar, P.O. Box 23874, Doha, Qatar

⁴ Institute of Physics, P.O. Box 57, 11001 Belgrade, Serbia

enhanced transport, and vector (gap) soliton formation (Jia and Fleischer 2009). Truncated rotating square waveguide arrays support localized modes that can exist even in the linear case (Zhang et al. 2016). The first experimental evidence of localization in nonlinear rotating structures was the photon tunneling in a twisted multicore fiber system that can display a chiral geometric phase accumulation, analogous to the Aharonov–Bohm effect (Parto et al. 2019). Recently, robust light bullets were demonstrated in strongly twisted fiber arrays pumped with ultrashort pulses (Milián et al. 2019).

On the other hand, edge states in a hexagonal array of helical waveguides are responsible for the photonic “topological insulation,” in which light that propagates along the edges of a photonic structure is topologically protected from the scattering on defects (Rechtsman et al. 2013; Lumer et al. 2013). The topological protection in “photonic graphene” was accomplished by making the waveguides helical; topological protection is impossible to accomplish for a wave packet populating a single site only (Lumer et al. 2013). Beam-splitting and adiabatic stabilization of light can be achieved in a periodically curved single-mode optical waveguide (Longhi et al. 2003). Adiabatic stabilization also exists in a three-dimensional waveguide with helicoidal axis bending; this phenomenon is the optical analogue of the adiabatic stabilization of a two-dimensional atom in a high-frequency and high-intensity circularly polarized laser field (Longhi 2005).

The starting point in understanding these interesting optical phenomena is the deep analogy between paraxial beam propagation in an optical waveguide with a bent axis and the single-electron dynamics in an atomic system (Longhi et al. 2003). The origin of this analogy is formal equivalence of the scalar paraxial beam propagation equation for the waveguide and the one-electron temporal Schrödinger equation represented in the Kramers–Henneberger (KH) reference frame (Henneberger 1968). The KH transformation is a transformation to the moving coordinate frame of the entirely free charged particle interacting with the applied electromagnetic field, and was first introduced in atomic physics to explore the interaction of a bound electron with superhigh intensity and high-frequency laser fields.

We considered stable and quasi-stable rotating solitons supported by a single spiraling waveguide in Petrović et al. (2018), Strinić et al. (2018). In our earlier publication (Petrović et al. 2018), we introduced the concept and the most important ideas of the variational approach (VA) to helical waveguides and illustrated the main challenges and problems. In this paper we will present the complete VA procedure for “slow” helical waveguiding in media with arbitrary nonlinearity.

2 Basic equations

We start from the most general paraxial wave equation for the beam propagation in a dielectric medium, which responds to light by changing its refractive index. In the steady state and three dimensions, the model equation in the dimensionless computational space is given by:

$$i \frac{\partial E}{\partial z} + \Delta E - V(x - x_0, y - y_0)E + \gamma F(I)E = 0, \quad (1)$$

where E is the slowly-varying beam envelope, Δ is the transverse Laplacian, $V(x - x_0, y - y_0)$ is an external potential, γ is the coupling constant, $I = |E|^2$ is the laser light intensity measured in units of the background intensity, and $F(I)$ is the nonlinearity.

The functions $x_0 = x_0(z) = \rho \cos(\Omega z)$, $y_0 = y_0(z) = \rho \sin(\Omega z)$ represent the helical waveguide, where ρ is the helix radius, Ω is the spatial frequency, and $\Lambda = 2\pi/\Omega$ is the period of rotation. A single spiral waveguide is presented in Fig. 1 (left).

We transform the coordinates and the electric field into a reference frame where the waveguide is straight, using the gauge transformation:

$$x \longrightarrow x' = x - x_0(z'), \quad x_0(z') = \rho \cos(\Omega z'), \tag{2}$$

$$y \longrightarrow y' = y - y_0(z'), \quad y_0(z') = \rho \sin(\Omega z'), \tag{3}$$

$$z \longrightarrow z', \tag{4}$$

$$E \longrightarrow E \exp \left[\frac{i}{2} x' \dot{x}_0(z) + \frac{i}{2} y' \dot{y}_0(z) + \frac{i}{4} \int_0^z \dot{x}_0^2(z') dz' + \frac{i}{4} \int_0^z \dot{y}_0^2(z') dz' \right], \tag{5}$$

where ' denotes the moving coordinate frame, and $\dot{f} = \frac{\partial f}{\partial z'}$. The governing Eq. (1) after the gauge transformation becomes:

$$i \frac{\partial E}{\partial z'} + \Delta' E - V_{\text{eff}}(x', y', z') E + \gamma F(I) E = 0, \tag{6}$$

with an effective potential

$$V_{\text{eff}}(x', y', z') = V(x', y') + \frac{1}{2} [x' \ddot{x}_0(z') + y' \ddot{y}_0(z')]. \tag{7}$$

We assume that the imprinted spiral waveguide profile is in the form of a Gaussian:

$$V(x', y') = -\alpha \exp(-x'^2/W^2 - y'^2/W^2), \tag{8}$$

with the “depth” α and the “width” W . Effective potential in the moving coordinate frame is presented in Fig. 1 (right).

If the next condition is satisfied:

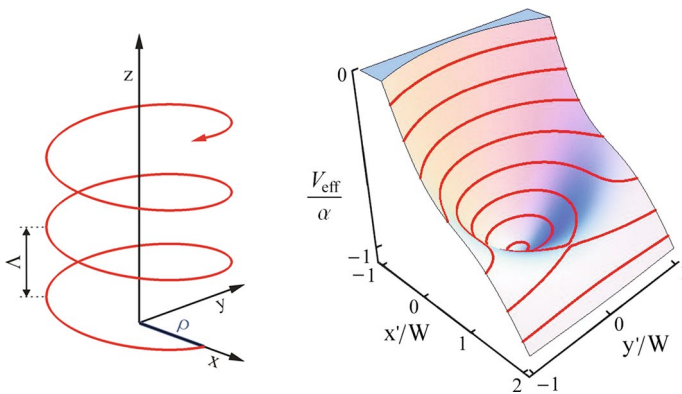


Fig. 1 Schematic picture of the spiral single waveguide (left). Effective potential in the moving coordinate frame for $\Omega z' = 0$ (right)

$$\beta = \frac{\rho W \Omega^2}{2\alpha} < \sqrt{\frac{2}{e}} \approx 0.86, \tag{9}$$

then the potential $V_{\text{eff}}(x', y', z')$ has a nonstationary minimum at $(x'_m(z'), y'_m(z'))$, where $|x'_m(z')|/W \leq 1/\sqrt{2} \approx 0.7$ and $|y'_m(z')|/W \leq 1/\sqrt{2} \approx 0.7$. We see that the potential barrier minimum rotates around the spiral waveguide center, where the radius of this circle $Q = \sqrt{x_m'^2 + y_m'^2}$ is given by the relation:

$$\beta = 2 \frac{Q}{W} \exp\left(-\frac{Q^2}{W^2}\right). \tag{10}$$

For smaller values of $\beta \ll 1$ we have $Q = \beta W/2$ (dashed line in Fig. 2 left). Effective potential profile for $\beta = 0.5$ at several different propagation distances is presented in Fig. 2 (right).

3 Variational approach

In order to better understand dynamical phenomena concerning beam propagation along a helical waveguide, we apply a powerful VA approximate technique (Aleksić et al. 2012). The idea is to decouple nonlinearity from the waveguide, which is possible in the shallow waveguide approximation.

The Lagrangian density corresponding to Eq. (6) is:

$$L = \frac{i}{2} \left(\frac{\partial E^*}{\partial z'} E - \frac{\partial E}{\partial z'} E^* \right) + |\nabla E|^2 + V_{\text{eff}}(x', y', z') |E|^2 - \gamma \int_0^{|E|^2} F(I) dI, \tag{11}$$

where the asterisk * denotes complex conjugate. An appropriate variation of Lagrangian yields Eq. (6) as the Euler–Lagrange equation.

After the transformation to the moving coordinate frame, we assume a Gaussian beam solution (whose parameters vary with z') in the Lagrangian density formalism, and make an ansatz:

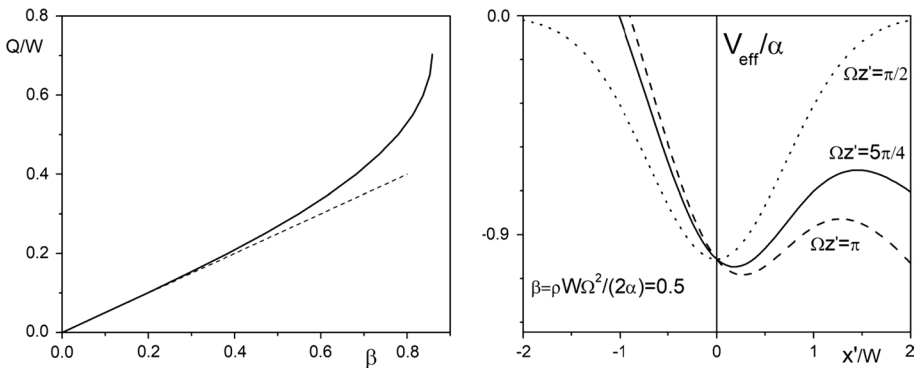


Fig. 2 The distance of potential minimum Q as a function of the parameter β , given by Eq. (10) (left). Effective potential profile for $\beta = 0.5$ and several different values of $\Omega z'$ (right)

$$E = A \exp \left[-\frac{(x' - X_C)^2}{2X^2} - \frac{(y' - Y_C)^2}{2Y^2} \right] \tag{12}$$

$$* \exp [iC_X(x' - X_C)^2 + iC_Y(y' - Y_C)^2 + iS_X(x' - X_C) + iS_Y(y' - Y_C) + i\Psi],$$

where A is the amplitude, X and Y are beam widths, (X_C, Y_C) is the transverse position of the beam's center, C_X and C_Y are the wave-front curvatures along x and y , S_X and S_Y are the drift velocity components, and Ψ is the nonlinear phase shift.

By substituting the trial functions into Eq. (11) and averaging Lagrangian over the transverse coordinates $\langle L \rangle = \int_{-\infty}^{+\infty} \int_{-\infty}^{+\infty} L dx' dy'$, one gets the following expression:

$$\langle L \rangle = P \left[\frac{\partial \Psi}{\partial z'} + \frac{1}{2} X^2 \left(4C_X^2 + \frac{\partial C_X}{\partial z'} \right) + \frac{1}{2} Y^2 \left(4C_Y^2 + \frac{\partial C_Y}{\partial z'} \right) \right] + P \left[S_X \left(S_X - \frac{\partial X_C}{\partial z'} \right) + S_Y \left(S_Y - \frac{\partial Y_C}{\partial z'} \right) + U(P, X, Y, X_C, Y_C) \right], \tag{13}$$

where $P = \pi A^2 XY$ is the beam power and

$$U = \frac{1}{2X^2} + \frac{1}{2Y^2} - \pi \frac{XY}{P} \gamma G \left(\frac{P}{\pi XY} \right) + U_1, \tag{14}$$

$$U_1 = -\frac{\alpha W^2 \exp \left(-\frac{X_C^2}{W^2 + X^2} - \frac{Y_C^2}{W^2 + Y^2} \right)}{\sqrt{(W^2 + X^2)(W^2 + Y^2)}} + \frac{1}{2} [X_C \ddot{x}_0(z') + Y_C \ddot{y}_0(z')], \tag{15}$$

is the potential, with the G term standing for the transformed nonlinearity,

$$G(A^2) = \frac{1}{\pi} \int dx' dy' \int_0^{A^2 \exp(-x'^2 - y'^2)} F(I) dI. \tag{16}$$

The set of explicit Euler–Lagrange equations can be derived under the condition that the variation with respect to each of the unknown functions should be zero, i.e. $\delta \langle L \rangle / \delta T = 0$ where $T \in \{P, X, Y, X_C, Y_C, C_X, C_Y, S_X, S_Y, \Psi\}$. After some algebra, one obtains the following set of ordinary differential equations:

$$\frac{dP}{dz'} = 0, \tag{17}$$

$$\frac{d^2 X}{dz'^2} = -4 \frac{\partial U}{\partial X}, \quad \frac{d^2 Y}{dz'^2} = -4 \frac{\partial U}{\partial Y}, \tag{18}$$

$$\frac{d^2 X_C}{dz'^2} = -2 \frac{\partial U}{\partial X_C}, \quad \frac{d^2 Y_C}{dz'^2} = -2 \frac{\partial U}{\partial Y_C}, \tag{19}$$

$$C_X = \frac{1}{4X} \frac{dX}{dz'}, \quad C_Y = \frac{1}{4Y} \frac{dY}{dz'}, \tag{20}$$

$$S_X = \frac{1}{2} \frac{dX_C}{dz'}, \quad S_Y = \frac{1}{2} \frac{dY_C}{dz'}, \tag{21}$$

$$\frac{d\psi}{dz'} = S_X^2 + S_Y^2 + \frac{\partial(PU)}{\partial P} + X^2 \frac{\partial U}{\partial X^2} + Y^2 \frac{\partial U}{\partial Y^2}. \tag{22}$$

The dynamics of the beam is described by the motion of a representative particle in a four-dimensional nonstationary potential. In general, analysis of the system of Eqs. (17)–(22) is very complicated.

The potential

$$U_1 = -\frac{\alpha W^2 \exp\left(-\frac{X_C^2}{W^2+X^2} - \frac{Y_C^2}{W^2+Y^2}\right)}{\sqrt{(W^2+X^2)(W^2+Y^2)}} - \frac{1}{2} \rho \Omega^2 [X_C \cos(\Omega z') + Y_C \sin(\Omega z')], \tag{23}$$

has a nonstationary minimum with respect to the variables X_C and Y_C at the point (X_{cm}, Y_{cm}) , where $|X_{cm}|/\sqrt{W^2+X^2} \leq 1/\sqrt{2} \approx 0.7$ and $|Y_{cm}|/\sqrt{W^2+Y^2} \leq 1/\sqrt{2} \approx 0.7$. By analogy with potential V_{eff} , given by Eqs. (7)–(8), we obtain the next conditions for the existence of potential minimum:

$$\delta_X = \beta \left(1 + \frac{X^2}{W^2}\right) \sqrt{1 + \frac{Y^2}{W^2}} < \sqrt{\frac{2}{e}} \approx 0.86, \tag{24}$$

$$\delta_Y = \beta \left(1 + \frac{Y^2}{W^2}\right) \sqrt{1 + \frac{X^2}{W^2}} < \sqrt{\frac{2}{e}} \approx 0.86. \tag{25}$$

The system of Eqs. (18)–(19) becomes:

$$\frac{d^2 X}{dz'^2} = 4 \left[\frac{1}{X^3} - \frac{\alpha W^2 (W^2 + X^2 - 2X_C^2)}{(W^2 + X^2)^{5/2} (W^2 + Y^2)^{1/2}} X - \gamma \frac{\Gamma(A^2)}{X} \right], \tag{26}$$

$$\frac{d^2 Y}{dz'^2} = 4 \left[\frac{1}{Y^3} - \frac{\alpha W^2 (W^2 + Y^2 - 2Y_C^2)}{(W^2 + Y^2)^{5/2} (W^2 + X^2)^{1/2}} Y - \gamma \frac{\Gamma(A^2)}{Y} \right], \tag{27}$$

$$\begin{aligned} \frac{d^2 X_C}{dz'^2} = & -\frac{4\alpha W^2 X_C}{(W^2 + X^2)^{3/2} (W^2 + Y^2)^{1/2}} \exp\left(-\frac{X_C^2}{W^2 + X^2} - \frac{Y_C^2}{W^2 + Y^2}\right) + \\ & + \rho \Omega^2 \cos(\Omega z'), \end{aligned} \tag{28}$$

$$\begin{aligned} \frac{d^2 Y_C}{dz'^2} = & -\frac{4\alpha W^2 Y_C}{(W^2 + Y^2)^{3/2} (W^2 + X^2)^{1/2}} \exp\left(-\frac{X_C^2}{W^2 + X^2} - \frac{Y_C^2}{W^2 + Y^2}\right) + \\ & + \rho \Omega^2 \sin(\Omega z'), \end{aligned} \tag{29}$$

where the function Γ is

$$\Gamma = \dot{G}(A^2) - \frac{G(A^2)}{A^2}. \tag{30}$$

In the linear approximation (where $\delta_x \ll 1$ and $\delta_y \ll 1$, and consequently $|X_{cm}|/W \ll 1$ and $|Y_{cm}|/W \ll 1$), Eqs. (26)–(29) are transformed into simpler ones:

$$\frac{d^2X}{dz'^2} = 4 \left[\frac{1}{X^3} - \frac{\alpha W^2 X}{(W^2 + X^2)^{3/2} (W^2 + Y^2)^{1/2}} - \gamma \frac{\Gamma(A^2)}{X} \right], \tag{31}$$

$$\frac{d^2Y}{dz'^2} = 4 \left[\frac{1}{Y^3} - \frac{\alpha W^2 Y}{(W^2 + Y^2)^{3/2} (W^2 + X^2)^{1/2}} - \gamma \frac{\Gamma(A^2)}{Y} \right], \tag{32}$$

$$\frac{d^2X_C}{dz'^2} = - \frac{4\alpha W^2 X_C}{(W^2 + X^2)^{3/2} (W^2 + Y^2)^{1/2}} + \rho \Omega^2 \cos(\Omega z'), \tag{33}$$

$$\frac{d^2Y_C}{dz'^2} = - \frac{4\alpha W^2 Y_C}{(W^2 + Y^2)^{3/2} (W^2 + X^2)^{1/2}} + \rho \Omega^2 \sin(\Omega z'). \tag{34}$$

We see from Eqs. (31)–(32) that the parameters for propagation of the axially-symmetric soliton with (constant) width $R = X = Y$ along the helical waveguide are determined by the relation:

$$\frac{1}{R^2} - \frac{\alpha W^2 R^2}{(W^2 + R^2)^2} - \gamma \Gamma(A^2) = 0. \tag{35}$$

The dynamics of the axially-symmetric soliton can be investigated from Eqs. (33)–(34). Transverse position of the beam’s center is described by the equations of a linear two-dimensional driven oscillator with the driving force frequency Ω :

$$\frac{d^2X_C}{dz'^2} = - \omega^2 X_C + \rho \Omega^2 \cos(\Omega z'), \tag{36}$$

$$\frac{d^2Y_C}{dz'^2} = - \omega^2 Y_C + \rho \Omega^2 \sin(\Omega z'), \tag{37}$$

where $\omega = 2\sqrt{\alpha}W/(W^2 + R^2) \gg \Omega$ is the characteristic frequency of the system.

4 Photorefractive nonlinearity

In photorefractive media, the nonlinearity is of the form $F(I) = \frac{I}{1+I}$. In this case, $G(A^2) = A^2 + Li_2(-A^2)$, where the dilogarithm function is defined in the integral form as $Li_2(z) = \int_z^0 \frac{\ln(1-t)}{t} dt$. The function Γ becomes:

$$\Gamma = \dot{G}(A^2) - \frac{G(A^2)}{A^2} = -\frac{\ln(1 + A^2) + Li_2(-A^2)}{A^2}, \tag{38}$$

and Eq. (35) has to be solved numerically. One must keep in mind that the space of parameters has to satisfy the following condition:

$$\delta = \beta \left(1 + \frac{R^2}{W^2} \right)^{3/2} < \sqrt{\frac{2}{e}} \approx 0.86. \tag{39}$$

The variational approach for the light propagating along a helical waveguide in media with the photorefractive type of nonlinearity is already presented in more details in Petrović et al. (2018).

5 Cubic-quintic nonlinearity

In case of the cubic-quintic nonlinearity, one has $F(I) = I(1 - I)$ and $G(A^2) = \frac{1}{36}(9 - 4A^2)A^2$. The function Γ is now:

$$\Gamma = \dot{G}(A^2) - \frac{G(A^2)}{A^2} = \frac{1}{36}(9 - 8A^2)A^2. \tag{40}$$

We see that, in contrast to the previous case, Eq. (35) can be solved analytically.

The comparison between numerical and approximate VA solution is presented in Fig. 3, where the most important fundamental soliton characteristics are shown. As already mentioned, the steady state does not exist in the dynamical case, but it is still possible to estimate soliton parameters using VA. In fact, there are two sets of zeros (two branches), but only the lower one (the lower branch) is stable; in Fig. 3 for both cases the stable branches are presented only. We note very good agreement between the results of variational approach and the numerical solitonic solutions.

We tested the stability of our solutions by direct numerical simulations of the beam propagation in a helically twisted optical waveguide formed in a medium with cubic-quintic

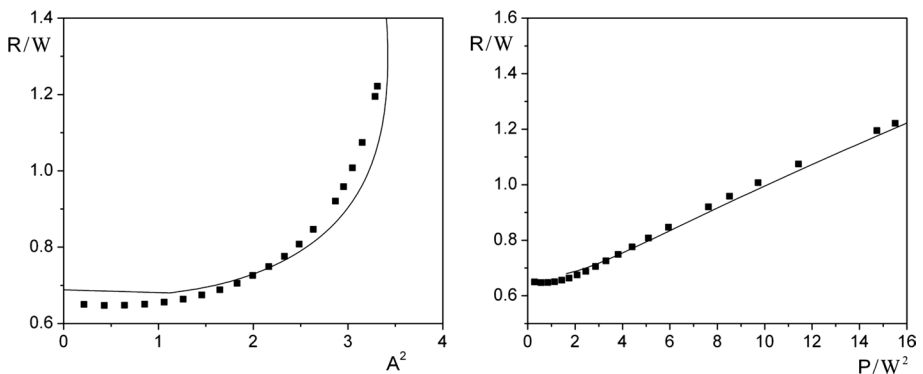


Fig. 3 Fundamental soliton beam width (scaled with waveguide width) as a function of the peak intensity (left) and scaled beam power (right). Black dots represent stable rotary solitonic solutions obtained numerically; black solid line represents results of the variational approach. Parameters: $\alpha W^2 = 10$, $\rho \Omega^2 W^3 = 0.1$, and $\gamma W^2 = 1$ ($W = 1$, $\alpha = 10$, $\rho = 2.5$, $\Omega = -0.2$, $\gamma = 1$)

nonlinearity. Numerical procedure for the investigation of the light propagation is the split-step beam propagation method based on the fast Fourier transform. We utilize the fourth-order symplectic algorithm. As expected, the behavior of spiraling spatial solitons supported by the 3D helical waveguide structure in a medium with cubic-quintic nonlinearity is very similar to the behavior of spiralling solitons in a medium with photorefractive nonlinearity (Petrović et al. 2018). They both perform robust and stable rotational-oscillatory motion over many rotation periods.

6 Conclusions

In this paper, we have presented a general variational approach for computing soliton parameters analytically, for light propagation in a single spiral waveguide formed in a nonlinear dielectric medium in the regime of low spatial frequency of the waveguide rotation. Our approach includes various types of nonlinearity. In the particular case of media with cubic-quintic nonlinearity, we have found that analytical expressions are in very good agreement with numerical findings.

Acknowledgements This work was supported by the Ministry of Science of the Republic of Serbia under the Projects OI 171033 and 171006, by the NPRP 11S-1126-170033 project of the Qatar National Research Fund, and the Russian Science Foundation Project No. 18-11-00247. Authors acknowledge supercomputer time provided by the IT Research Computing group of Texas A&M University at Qatar. MRB acknowledges support by the Al Sraiya Holding Group.

References

- Aleksić, N., Petrović, M., Strinić, A., Belić, M.: Solitons in highly nonlocal nematic liquid crystals: variational approach. *Phys. Rev. A* **85**, 033826 (2012)
- Cuevas, J., Malomed, B., Kevrekidis, P.G.: Two-dimensional discrete solitons in rotating lattices. *Phys. Rev. E* **76**, 046608 (2007)
- Henneberger, W.C.: Perturbation method for atoms in intense light beams. *Phys. Rev. Lett.* **21**, 838–841 (1968)
- Jia, S., Fleischer, J.: Nonlinear light propagation in rotating waveguide arrays. *Phys. Rev. A* **79**, 041804 (R) (2009)
- Kivshar, Y.S., Agrawal, G.: *Optical Solitons: From Fibers to Photonic Crystals*. Academic, San Diego (2003)
- Longhi, S.: Wave packet dynamics in a helical optical waveguide. *Phys. Rev. A* **71**, 055402 (2005)
- Longhi, S.: Bloch dynamics of light waves in helical optical waveguide arrays. *Phys. Rev. B* **76**, 195119 (2007)
- Longhi, S., Janner, D., Marano, M., Laporta, P.: Quantum-mechanical analogy of beam propagation in waveguides with a bent axis: dynamic-mode stabilization and radiation-loss suppression. *Phys. Rev. E* **67**, 036601 (2003)
- Lumer, Y., Plotnik, Y., Rechtsman, M., Segev, M.: Self-localized states in photonic topological insulators. *Phys. Rev. Lett.* **111**, 243905 (2013)
- Milián, C., Kartashov, Y.V., Torner, L.: Robust ultrashort light bullets in strongly twisted waveguide arrays. *Phys. Rev. Lett.* **123**, 133902 (2019)
- Parto, M., Lopez-Aviles, H., Antonio-Lopez, J.E., Khajavikhan, M., Amezcua-Correa, R., Christodoulides, D.N.: Observation of twist-induced geometric phases and inhibition of optical tunneling via Aharonov–Bohm effects. *Sci. Adv.* **5**, 1–5 (2019)
- Petrović, M.S., Strinić, A.I., Aleksić, N.B., Belić, M.R.: Rotating solitons supported by a spiral waveguide. *Phys. Rev. A* **98**, 063822 (2018)
- Rechtsman, M., Zeuner, J., Plotnik, Y., Lumer, Y., Podolsky, D., Dreisow, F., Nolte, S., Segev, M., Szameit, A.: Photonic Floquet topological insulators. *Nature* **496**, 196–200 (2013)

- Sakaguchi, H., Malomed, B.: Solitary vortices and gap solitons in rotating optical lattices. *Phys. Rev. A* **79**, 043606 (2009)
- Strinić, A.I., Petrović, M.S., Aleksić, N.B., Belić, M.R.: Quasi-stable rotating solitons supported by a single spiraling waveguide. *Opt. Quant. Electron.* **50**, 126 (2018)
- Zhang, X., Ye, F., Kartashov, Y., Vysloukh, V., Chen, X.: Localized waves supported by the rotating waveguide array. *Opt. Lett.* **41**, 4106–4109 (2016)

Publisher's Note Springer Nature remains neutral with regard to jurisdictional claims in published maps and institutional affiliations.